Original Article

# Predictive Ability of Galilei to Distinguish Subclinical Keratoconus and Keratoconus from Normal Corneas

**Sepehr Feizi[1], MD, MS; Mehdi Yaseri[2,3], PhD; Bahareh Kheiri[3], MS**

[1]*Ocular Tissue Engineering Research Center, Shahid Beheshti University of Medical Sciences, Tehran, Iran*
[2]*Department of Epidemiology and Biostatistics, Tehran University of Medical Sciences, Tehran, Iran*
[3]*Ophthalmic Research Center, Shahid Beheshti University of Medical Sciences, Tehran, Iran*

## Abstract

**Purpose:** To determine the predictive ability of different data measured by the Galilei dual Scheimpflug analyzer in differentiating subclinical keratoconus and keratoconus from normal corneas.
**Methods:** This prospective comparative study included 136 normal eyes, 23 eyes with subclinical keratoconus, and 51 keratoconic eyes. In each eye, keratometric values, pachymetry, elevation parameters and surface indices were evaluated. Receiver operating characteristic (ROC) curves were calculated and quantified by using the area under the curve (AUC) to compare the sensitivity and specificity of the measured parameters and to identify optimal cutoff points for differenciating subclinical keratoconus and keratoconus from normal corneas. Several model structures including keratometric, pachymetric, elevation parameters and surface indices were analyzed to find the best model for distinguishing subclinical and clinical keratoconus. The data sets were also examined using the non-parametric "classification and regression tree" (CRT) technique for the three diagnostic groups.
**Results:** Nearly all measured parameters were strong enough to distinguish keratoconus. However, only the radius of best fit sphere and keratometry readings had an acceptable predictive accuracy to differentiate subclinical keratoconus. Elevation parameters and surface indices were able to differentiate keratoconus from normal corneas in 100% of eyes. Meanwhile, none of the parameter sets could effectively discriminate subclinical keratoconus; a 3-factor model including keratometric variables, elevation data and surface indices provided the highest predictive ability for this purpose.
**Conclusion:** Surface indices measured by the Galilei analyzer can effectively differentiate keratoconus from normal corneas. However, a combination of different data is required to distinguish subclinical keratoconus.

**Keywords:** Galilei Dual Scheimpflug Analyzer; Keratoconus; Subclinical Keratoconus

*J Ophthalmic Vis Res* 2016; 11 (1): 8-16.

**Correspondence to:**
Sepehr Feizi, MD, MS. Ocular Tissue Engineering Research Center, Shahid Beheshti University of Medical Sciences, No. 23, Paidarfard St., Boostan 9 St., Pasdaran Ave., Tehran 16666, Iran.
E-mail: sepehrfeizi@yahoo.com

Received: 05-01-2014 Accepted: 28-06-2014

Access this article online

Quick Response Code:

Website: www.jovr.org

DOI: 10.4103/2008-322X.180707

## INTRODUCTION

The terms forme fruste keratoconus, subclinical keratoconus and keratoconus suspect have been used to designate early stages of keratoconus which do not become manifest on biomicroscopy, but demonstrate



**How to cite this article:** Feizi S, Yaseri M, Kheiri B. Predictive ability of galilei to distinguish subclinical keratoconus and keratoconus from normal corneas. J Ophthalmic Vis Res 2016;11:8-16.

subtle topographic features comparable to those of clinical keratoconus.[1-3] Studies suggest that subclinical or clinical keratoconus is found in 1 to 6% of myopic patients undergoing refractive surgery.[4-7] Several corneal imaging techniques have evolved, mainly to distinguish subclinical or clinical keratoconus among patients scheduled for refractive surgery because operation on an undetected keratoconic cornea is a major cause of post-refractive surgery ectasia.[8]

Placido disk-based videokeratography which examines the central 7-8 mm of the anterior corneal surface is the initial technique most widely used for diagnosis of keratoconus.[5,9,10] The second introduced technique was slit scanning topography (Orbscan, Bausch and Lomb, Orbtek Inc., Salt Lake City, UT, USA) followed by Scheimpflug camera (Pentacam Comprehensive Eye Scanner, Oculus Optikgerte GmbH, Wetzlar, Germany) which are able to measure anterior and posterior corneal surface elevation data and determine pachymetry maps.[11,12]

The more recently introduced Galilei dual Scheimpflug system (Ziemer Ophthalmic System AG, Port, Switzerland) is a noninvasive diagnostic instrument designed for the analysis of anterior segment characteristics including Placido disk-based topography, pachymetry, net corneal power, elevation maps, anterior chamber depth and corneal wavefront.[11,12] It combines two technologies including Placido imaging which provides curvature data, and Scheimpflug imaging which is optimal for precise elevation measurements. In contrast to other imaging techniques such as Orbscan, the information regarding what constitutes normal or abnormal values measured with the Galilei dual Scheimpflug analyzer is limited. Moreover, values and indices obtained from different instruments are rarely interchangeable as these instruments use different methods to depict corneal surfaces. Therefore, it is of high significance to determine the abnormal values of the parameters obtained by the Galilei dual Scheimpflug analyzer.

The purpose of the present study was to measure and compare keratometric, pachymetric, and elevation parameters as well as corneal surface indices among eyes with subclinical keratoconus, keratoconus, and normal corneas using the Galilei dual Scheimpflug camera and to determine their predictive ability for detection of these conditions. Furthermore, an attempt was made to identify optimal cutoff points for these parameters to maximize sensitivity and specificity in differentiating subclinical keratoconus and keratoconus from normal corneas.

## METHODS

This prospective comparative study included 136 normal right eyes of 136 refractive surgery candidates (58 male cases), 23 eyes of 23 subjects with subclinical keratoconus (18 male patients), and 51 eyes of 48 patients with keratoconus (29 male cases).

The diagnosis of subclinical keratoconus and keratoconus was based on clinical slit lamp findings (stromal thinning, conical protrusion, Fleischer ring, and Vogt`s striae) and characteristic patterns based on Placido disk corneal topography (Tomey, EM-3000, version 4.20, Nagoya, Japan). These findings were divided into minor and major criteria. Major criteria consisted of abnormal biomicroscopic findings including Vogt's striae and Fleischer ring >2 mm, as well as abnormal topographic indices including skewed radial axis (SRAX) >21°, keratoconus predicting index (KPI) >30%, keratoconus severity index (KSI) >30%, and abnormal keratoconus index (KCI). Minor criteria included asymmetric bow-tie pattern without SRAX, inferior steepening, KPI of 23-30% and KSI of 15-30%.

Patients who had one abnormal biomicroscopic finding and one major or two minor criteria were diagnosed with keratoconus. Subjects with a normal appearing cornea and one major or two minor topographic criteria was diagnosed with subclinical keratoconus. Normal subjects demonstrated no major criteria and no or only one minor criterion.[13] Keratoconic eyes were divided into 3 groups according to mean keratometry (K) readings: Mild ($K \leq 47.0$ D; 15 eyes), moderate ($47.0 \text{ D} < K < 52.0$ D; 15 eyes), and severe ($K \geq 52.0$ D; 21 eyes).

Eyes with previous acute corneal hydrops or a history of any ocular surgery were excluded. In the normal group, the only ocular problem was refractive error, and any ocular pathology such as dry eye, glaucoma, retinal disease, prior ocular surgery, or systemic diseases such as diabetes and connective tissue disorders led to exclusionof the subject. All participants were asked to stop wearing soft contact lenses for at least two weeks and rigid gas-permeable contact lenses for at least four weeks before measurements.

A signed informed consent was obtained after explaining the purpose of the study, and the study was approved by the Institutional Review Board of the Ophthalmic Research Center, affiliated to Shahid Beheshti University of Medical Sciences, Tehran, Iran.

A complete ocular examination including slit lamp biomicroscopy, cycloplegic refraction, corrected distance visual acuity (CDVA) using Snellen acuity chart, keratometry readings, intraocular pressure measurement, and dilated fundus examination was performed.

For measurements with the Galilei dual Scheimpflug analyzer, participants were seated with their chin on a chinrest and forehead against the forehead strap while fixating on the target. Appropriate alignment of the scan center with the corneal apex was checked using an initial Scheimpflug image formed on the monitor, together with a guide line. Measurement results were checked under a

quality-specification window; only measurements with an "OK" reading were enrolled. If the comments were marked yellow or red (i.e., not OK), the examination would be repeated. Four groups of data were then used for statistical analysis. These groups consisted of (1) keratometry values including power of the flat ($K_f$) and steep ($K_s$) meridians, keratometric astigmatism and mean keratometry, (2) pachymetry values including central and minimal (at the thinnest point) corneal thickness, (3) elevation parameters including the radius of anterior and posterior best-fit sphere (BFS) and the maximum anterior and posterior elevations in the central 3, 5 and 7 mm zones of the cornea, and (4) surface indices including inferior-superior index (I-S), standard deviation of corneal power (SDP), surface regularity index (SRI), surface asymmetry index (SAI), irregular astigmatism index (IAI), differential sector index (DSI), opposite sector index (OSI), center/surround index (CSI), keratoconus prediction index (KPI), and keratoconus probability (KProb).

For maximum corneal elevation, a best-fit sphere (BFS) was generated by the software, with the floating option over an 8-mm fit. The float map means that the reference body has no fixed center and the distance between the cornea and the sphere surface is optimized to be as small as possible. Anterior elevation was determined by taking the maximum difference in anterior elevation between best-fit sphere and patient's cornea. The posterior elevation was determined by taking the maximum difference in posterior elevation between best-fit sphere and patient`s cornea. All measurements were obtained by an experienced operator using the same machine and procedures.

All statistical analyses were performed using SPSS software version 17.0 (SPSS Inc., Chicago, IL, USA). General data including age, spherical equivalent refraction (SE), and keratometry readings as well as data obtained with the Galilei dual Scheimpflug analyzer were expressed as mean ± standard deviation (SD). One-way analysis of variance was used to compare these measurements between the study groups. In order to distinguish subclinical and clinical keratoconus from normal eyes, receiver operating characteristics (ROC) curves were calculated and quantified using the area under the curve (AUC) for different indices. Optimal cutoff points to distinguish subclinical keratoconus and keratoconus from normal corneas were calculated for the measured parameters. Positive likelihood ratio (sensitivity/[1-specificity]), and negative likelihood ratio ([1-sensitivity]/specificity) for these cutoff points were determined. *P* values less than 0.05 was considered as statistically significant.

Logistic regression analysis was performed to investigate predictors of keratometric, pachymetric and elevation data, and surface indices with calculation of $R^2$ and positive and negative predictive values. This analysis was used to examine several model structures. Each model was constructed of variables representing keratometric values, pachymetric parameters, elevation data, and/or surface indices. During our analysis, different models (assuming 1-, 2-, or 3-parameter sets) were tested and the best fitted-model was selected by values of fit indices.

Classification and regression trees (CRT) analysis was performed to identify useful tree-structures for classification of data from several groups. CRT is a stepwise, nonparametric procedure which assesses the classification potential of variables relative to a split or cutoff point. The single best predictor (the one whose optimal cutoff point maximizes the number of correct classifications among the diagnostic categories) is selected as the starting variable at the top of a hierarchical tree. Subjects with values less than the cutoff point move to one category, while those with values greater than the cutoff point move into a second box of the hierarchical tree. Cutoff points are then assessed in a step-wise fashion for the remaining predictors. A classification tree is generated and will grow until maximal classification is achieved or further splitting is judged as ineffective.

## RESULTS

Mean patient age was 28.6 ± 4.8 (range, 20-40) years in the normal group, 27.4 ± 3.2 (range, 21-39) years in subjects with subclinical keratoconus and 30.7 ± 5.7 (range, 19-40) years in patients with keratoconus ($P = 0.18$). CDVA was comparable between normal subjects (0.0 ± 0.11 logMAR) and those with subclinical keratoconus (0.04 ± 0.12 logMAR, $P = 0.68$). CDVA was significantly lower in the keratoconus group (0.34 ± 0.28 logMAR) as compared to normal subjects ($P < 0.001$) and subjects with subclinical keratoconus ($P < 0.001$). Similarly, there was no significant difference between normal eyes and those with subclinical keratoconus in terms of spherical equivalent refraction (-2.67 ± 0.23 and -3.40 ± 2.96 D, respectively; $P = 0.51$), which was significantly higher in the keratoconus group (-6.07 ± 5.2 D; $P < 0.001$). Table 1 compares the measured variables by the Galilei dual Scheimpflug analyzer among the study groups.

Tables 2 and 3 demonstrate AUC, the optimal cutoff points and their sensitivity, specificity, and positive and negative likelihood ratios for different parameter sets to distinguish eyes with keratoconus and subclinical keratoconus from normal eyes. As indicated, all parameters were strong enough (AUC > 0.80) to differentiate keratoconus. These values were less effective to distinguish eyes with subclinical keratoconus from normal eyes, and only the radius of the anterior and posterior BFS, and flat and mean keratometry readings had acceptable power for differentiation.

The results of logistic regression analysis demonstrated that both surface indices and elevation data had a

**Table 1. Comparisons of different data measured between the study groups**

| Variables | Normal | Subclincal keratoconus | Keratoconus | $P^{\dagger}$ | $P^{\ddagger 1}$ | $P^{\ddagger 2}$ |
|---|---|---|---|---|---|---|
| Mean keratometry (D) | 43.86±1.06 | 45.71±1.65 | 51.27±5.57 | <0.001 | 0.011 | <0.001 |
| Steep keratometry (D) | 44.52±1.24 | 46.64±2.17 | 54.15±8.45 | <0.001 | 0.062 | <0.001 |
| Flat keratometry (D) | 43.19±1.12 | 44.79±1.41 | 48.34±4.36 | <0.001 | 0.006 | <0.001 |
| Keratometric astigmatism (D) | 1.33±1 | 1.85±1.57 | 5.22±2.93 | <0.001 | 0.327 | <0.001 |
| Central corneal thickness (microns) | 568.44±34.19 | 555.65±39.66 | 496.98±37.2 | <0.001 | 0.210 | <0.001 |
| Minimal corneal thickness (microns) | 557.81±34.15 | 543.26±39.4 | 472.88±40.72 | <0.001 | 0.147 | <0.001 |
| Inferior-superior index (D) | 0.74±0.64 | 1.12±1.01 | 7.95±4.96 | <0.001 | 0.747 | <0.001 |
| Surface asymmetry index (D) | 0.55±0.26 | 0.8±0.49 | 5.18±3.98 | <0.001 | 0.812 | <0.001 |
| Surface regularity index (D) | 0.77±0.3 | 0.98±0.37 | 2.02±0.56 | <0.001 | 0.028 | <0.001 |
| Irregular astigmatism index (D) | 0.46±0.08 | 0.52±0.12 | 1.19±0.86 | <0.001 | 0.798 | <0.001 |
| Keratoconus prediction index (%) | 2.32±4.87 | 9.4±10.92 | 80.7±25.63 | <0.001 | 0.044 | <0.001 |
| Differential sector index (D) | 1.8±0.87 | 2.46±1.37 | 11.13±9.25 | <0.001 | 0.830 | <0.001 |
| Opposite sector index (D) | 0.77±0.54 | 1.23±0.94 | 9.15±8.46 | <0.001 | 0.858 | <0.001 |
| Center/surround index (D) | 0.33±0.21 | 0.5±0.57 | 3.66±2.82 | <0.001 | 0.830 | <0.001 |
| Standard deviation of corneal power (D) | 0.8±0.29 | 1.1±0.54 | 5.09±3.54 | <0.001 | 0.690 | <0.001 |
| Keratoconus probability (%) | 2.87±7.83 | 11.63±19.45 | 93.7±17.74 | <0.001 | 0.004 | <0.001 |
| Radius of anterior best-fit sphere (mm) | 7.75±0.19 | 7.47±0.25 | 7.1±0.56 | <0.001 | <0.001 | <0.001 |
| Radius of posterior best-fit sphere (mm) | 6.46±0.18 | 6.19±0.18 | 5.83±0.43 | <0.001 | <0.001 | <0.001 |
| Maximum anterior elevation in 3 mm zone (microns) | 4.81±3.1 | 6.91±4.68 | 29.78±29.57 | <0.001 | 0.775 | <0.001 |
| Maximum posterior elevation in 3 mm zone (microns) | 9.61±3.93 | 12.52±3.99 | 54.37±36.93 | <0.001 | 0.733 | <0.001 |
| Maximum anterior elevation in 5 mm zone (microns) | 7.6±5.66 | 10.17±7.15 | 36.31±56.37 | <0.001 | 0.899 | <0.001 |
| Maximum posterior elevation in 5 mm zone (microns) | 15.39±7.29 | 17.57±6.07 | 60.78±58.1 | <0.001 | 0.932 | <0.001 |
| Maximum anerior elevation in 7 mm zone (microns) | 16.16±9.62 | 20±14.36 | 67.65±91.49 | <0.001 | 0.915 | <0.001 |
| Maximum posterior elevation in 7 mm zone (microns) | 27.89±12.91 | 31±15.06 | 120.88±195.94 | <0.001 | 0.987 | <0.001 |

D, diopter; mm, millimeter. †Based on Analysis of Variance; ‡Adjusted for multiple comparisons based on Dunnett test; ‡1 Comparison between normal and subclinical keratoconus; ‡2 Comparison between normal and keratoconus

predictive ability of 100% to distinguish keratoconus from normal [Table 4]. In the subclinical keratoconus group, however, none of the variables could completely detect patients and the most representative variable set was elevation data set ($R^2$ = 0.60), followed by keratometric data set ($R^2$ = 0.40), surface indices set ($R^2$ = 0.39), and pachymetric set ($R^2$ = 0.15). A 3-factor model constructed of variables representing keratometric values, elevation data, and surface indices showed the best fit ($R^2$ = 0.68, positive predictive values, 83.3%, negative predictive values, 97.7%) among the structures analyzed to distinguish subclinical keratoconus from normal [Table 5].

CRT analysis on the entire data sets produced the decision tree shown in Figure 1. The parameters identified were SAI in layer 1 and the radius of posterior BFS in layer 2. Keratoconus was best discriminated from normal by SAI (99.4% correctly classified; $P < 0.001$; sensitivity, 100%; specificity, 99.3%; positive predictive value, 98.1%; negative predictive value, 100%). Subclinical keratoconus was best discriminated from normal with a two-step tree containing SAI in layer 1, and radius of posterior BFS in layer 2 (73.9% correct classification; $P < 0.001$). These combined results were associated with a sensitivity of 100%; specificity of 91.3%; positive predictive value of 43.4%; and negative predictive value of 100%.

Applying SAI > 1.28 to node 0 containing all study groups classified one normal eye, 4 eyes with subclinical keratoconus, and all eyes with keratoconus to node 2 [Figure 1]. Applying the radius of posterior BFS ≤6.175 mm to the remaining participants in node 1 categorized 4 normal eyes and 13 eyes with subclinical keratoconus to node 3. The CRT analysis could not further split the participants left in node 4, as the number of eyes with subclinical keratoconus was small. Cutoff points determined by CRT (SAI = 1.28 and radius of BFS = 6.175) were slightly different from those presented in Tables 1 and 2. This is because this analysis used cutoff values for both subclinical and clinical keratoconus versus normal corneas.

## DISCUSSION

The range and normal values of corneal tomographic parameters obtained by the Galilei dual Scheimpflug analyzer have previously been reported.[14,15] The current study reports the characteristics of four groups of parameters including topographic, keratometric, pachymetric, and elevation values measured with the Galilei dual Scheimpflug analyzer in eyes with subclinical keratoconus and keratoconus and compares these values with those in normal corneas.

**Table 2. Area under the curve cut-off points, and their sensitivity, specificity and positive and negative likelihood ratios for variables measured by the Galilei to distinguish eyes with subclinical keratoconus from control subjects**

| Variable | AUC | Cut-off | Sensitivity (%) | Specificity (%) | LR⁺ | LR⁻ |
|---|---|---|---|---|---|---|
| Radius of posterior best-fit sphere* (mm) | 0.892 | 6.27 | 87.0 | 87.1 | 6.74 | 0.15 |
| Flat keratometry (D) | 0.840 | 43.8 | 82.6 | 72.9 | 3.05 | 0.24 |
| Mean keratometry (D) | 0.833 | 45.49 | 65.2 | 94.7 | 12.30 | 0.37 |
| Radius of anterior best-fit sphere* (mm) | 0.828 | 7.645 | 82.6 | 69.7 | 2.73 | 0.25 |
| Steep keratometry (mm) | 0.805 | 46.4 | 61 | 93 | 9.13 | 0.42 |
| Maximum posterior elevation in 3 mm zone (microns) | 0.718 | 11.5 | 60.9 | 77.4 | 2.69 | 0.51 |
| Keratoconus prediction index (%) | 0.710 | 5.0 | 56.5 | 83.5 | 3.42 | 0.52 |
| Standard deviation of corneal power (D) | 0.692 | 1.065 | 56.5 | 85.7 | 3.95 | 0.51 |
| Surface regularity index (D) | 0.679 | 0.735 | 82.6 | 51.1 | 1.69 | 0.34 |
| Maximum anterior elevation in 3 mm zone (microns) | 0.678 | 3.5 | 87.0 | 43.6 | 1.54 | 0.30 |
| Keratoconus probability (%) | 0.669 | 11.6 | 39.1 | 95.5 | 8.69 | 0.64 |
| Irregular astigmatism index (D) | 0.664 | 0.445 | 73.9 | 54.1 | 1.61 | 0.48 |
| Differential sector index (D) | 0.646 | 1.725 | 73.9 | 55.6 | 1.66 | 0.47 |
| Surface asymmetry index (D) | 0.644 | 0.895 | 43.5 | 91.7 | 5.24 | 0.62 |
| Opposite sector index (D) | 0.637 | 1.85 | 30.4 | 98.5 | 20.27 | 0.71 |
| Maximum posterior elevation in 5 mm zone (microns) | 0.619 | 12.5 | 91.3 | 38.3 | 1.48 | 0.23 |
| Maximum anterior elevation in 5 mm zone (microns) | 0.615 | 4.5 | 82.6 | 36.1 | 1.29 | 0.48 |
| Minimal corneal thickness* (microns) | 0.604 | 525 | 43.5 | 82.6 | 2.50 | 0.68 |
| Inferior-superior index (D) | 0.597 | 1.6 | 34.8 | 89.5 | 3.31 | 0.73 |
| Keratometric astigmatism (D) | 0.589 | 1.355 | 56.5 | 65.4 | 1.63 | 0.67 |
| Central corneal thickness* (microns) | 0.584 | 534.5 | 43.5 | 83.3 | 2.60 | 0.68 |
| Maximum anterior elevation in 7 mm zone (microns) | 0.543 | 20.5 | 43.5 | 76.7 | 1.87 | 0.74 |
| Maximum posterior elevation in 7 mm zone (microns) | 0.539 | 39.5 | 30.4 | 87.2 | 2.38 | 0.80 |
| Center/surround index (D) | 0.534 | 0.99 | 21.7 | 100.0 | NE | 0.78 |

*Subclinical keratoconus is identified by values less than the specified cut-off points. mm, millimeter; D, diopter; AEC, area under the curve; LR, likhood ratio; NE, not evaluable; AUC, area under the curve

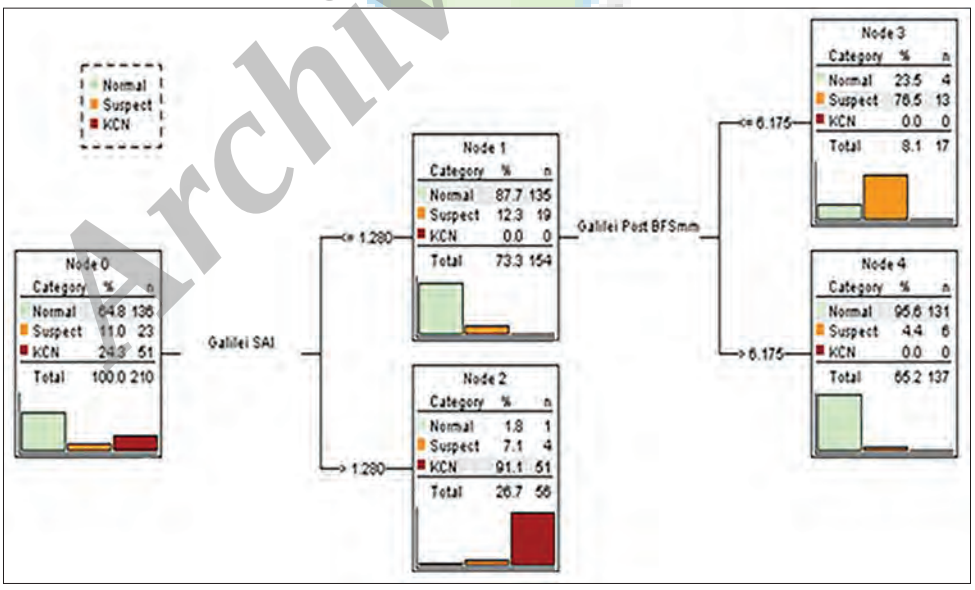


**Figure 1.** Classification and regression tree for three diagnostic groups. Percentages and numbers in each node of the tree refer to the proportion of the diagnostic groups which are identified by the decision tree.

Several technologies have been introduced to evaluate features of the corneal surface in normal and keratoconic corneas including Placido disk-based topography, slit scanning topography (Orbscan), and Scheimpflug system analyzer (Pentacam and Galilei).[1-3,11,12,16-21] As the Galilei dual Scheimpflug analyzer generates data differently as compared to the Orbscan and Pentacam, the cutoff points obtained

**Table 3. Area under the curve cut-off points and their sensitivity specificity, and positive and negative likelihood ratios for variables measured by the Galilei dual scheimpflug analyzer to distinguish eyes with keratoconus from control subjects**

| Variable | AUC | Cut-off | Sensitivity (%) | Specificity (%) | LR⁺ | LR⁻ |
|---|---|---|---|---|---|---|
| Keratoconus prediction index (%) | 0.999 | 18.55 | 100 | 99 | 133 | 0 |
| Surface asymmetry index (D) | 0.999 | 1.25 | 100 | 99 | 133 | 0 |
| Keratoconus probability (%) | 0.998 | 25.55 | 98 | 99 | 130.3 | 0.02 |
| Maximum posterior elevation in 3 mm zone (microns) | 0.993 | 18.5 | 96 | 96 | 25.5 | 0.04 |
| Standard deviation of corneal power (D) | 0.993 | 1.93 | 92 | 100 | NE | 0.08 |
| Opposite sector index (D) | 0.988 | 2.04 | 96 | 99 | 127.7 | 0.04 |
| Maximum anterior elevation in 3 mm zone (microns) | 0.982 | 12.5 | 90 | 97 | 29.9 | 0.1 |
| Surface regularity index (D) | 0.982 | 1.52 | 90 | 100 | NE | 0.1 |
| Differential sector index (D) | 0.977 | 3.26 | 98 | 91 | 10.9 | 0.02 |
| Irregular astigmatism index (D) | 0.974 | 0.58 | 92 | 92 | 11.1 | 0.09 |
| Inferior-superior index (D) | 0.971 | 2.33 | 90 | 98 | 59.9 | 0.1 |
| Steep keratometry (D) | 0.969 | 46.76 | 92 | 98 | 41.5 | 0.08 |
| Maximum posterior elevation in 5 mm zone (microns) | 0.962 | 22.5 | 92 | 89 | 8.2 | 0.09 |
| Mean keratometry (D) | 0.956 | 45.05 | 90 | 91 | 10 | 0.11 |
| Center/surround index (D) | 0.951 | 0.7 | 92 | 95 | 20.4 | 0.08 |
| Maximum anterior elevation in 5 mm zone (microns) | 0.948 | 12.5 | 90 | 86 | 6.7 | 0.12 |
| Maximum posterior elevation in 7 mm zone (microns) | 0.941 | 49.0 | 88 | 94 | 14.6 | 0.13 |
| Minimal corneal thickness* (microns) | 0.939 | 519.0 | 92 | 88 | 7.6 | 0.1 |
| Radius of posterior best-fit sphere* (mm) | 0.937 | 6.28 | 92 | 87 | 7.1 | 0.1 |
| Maximum anterior elevation in 7 mm zone (microns) | 0.920 | 27.5 | 88 | 87 | 6.9 | 0.14 |
| Central corneal thickness* (microns) | 0.910 | 537.5 | 92 | 80 | 4.6 | 0.11 |
| Keratometric astigmatism (D) | 0.896 | 2.84 | 82 | 91 | 9.1 | 0.2 |
| Radius of anterior best-fit sphere* (mm) | 0.890 | 7.38 | 70 | 100 | NE | 0.3 |
| Flat keratometry (D) | 0.878 | 45.64 | 72 | 100 | NE | 0.28 |

*Keratoconus is identified by values less than the specified cut-off points. mm, millimeter; D, diopter; AEC, area under the curve; LR, likhood ratio; NE, not evaluable; AUC, area under the curve

**Table 4. Predictive ability of different data sets to differentiate subclinical keratoconus and keratoconus from normal eyes**

| | Elevation data | Surface indices data | Pachymetric data | Keratometric data |
|---|---|---|---|---|
| Subclinical keratoconus | | | | |
| $R2^{\dagger}$ | 0.6 | 0.39 | 0.15 | 0.41 |
| AUC | 0.92 | 0.86 | 0.75 | 0.84 |
| Sensitivity (%) | 83 | 83 | 87 | 65 |
| Specificity (%) | 98 | 78 | 54 | 94 |
| LR⁺ | 35.8 | 3.7 | 1.9 | 10.6 |
| LR⁻ | 0.2 | 0.2 | 0.2 | 0.4 |
| Keratoconus | | | | |
| $R^{2\dagger}$ | 1 | 1 | 0.91 | 0.85 |
| AUC | 1 | 1 | 0.99 | 0.97 |
| Sensitivity (%) | 100 | 100 | 93 | 91 |
| Specificity (%) | 100 | 100 | 100 | 98 |
| LR⁺ | NE | NE | NE | 39.6 |
| LR⁻ | NE | NE | 0.1 | 0.1 |

†Based on binomial logistic regression, $R^2$, Nagelkerke Pseudo $R^2$; AUC, area under the curve; LR, likelihood ratio; NE, not evaluable; AUC, area under the curve

by these instruments cannot be used interchangeably. For instance, the cutoff value for maximum posterior elevation in the central 5 mm of the keratoconus cornea (the area which has been widely reported) was 22.5 µm in the present study. This value is much lower than the corresponding measurements obtained with the Pentacam (35 µm[1,21] and 55.8 µm[22]) and Orbscan II (40.0 µm[19,20] and 48.5 µm[21]). This finding explains the reason for which we studied the tomographic features of the corneal surface in these conditions

**Table 5. Predictive ability of different model structures to differentiate subclinical keratoconus from normal eyes**

| | $R^2$ | AUC | Sensitivity (%) | Specificity (%) | $LR^+$ (%) | $LR^-$ (%) |
|---|---|---|---|---|---|---|
| Two-model structure | | | | | | |
| Elevation + surface indices data | 0.64 | 0.933 | 93.8 | 80.8 | 13.9 | 10.3 |
| Elevation + keratometric data | 0.64 | 0.923 | 98.4 | 81.1 | 17.7 | 10.3 |
| Elevation + pachymetric data | 0.43 | 0.924 | 97.7 | 80.3 | 17.8 | 10.3 |
| Surface indices + keratometric data | 0.6 | 0.921 | 86.0 | 77.4 | 10.1 | 10.3 |
| Surface indices + pachymetric data | 0.6 | 0.828 | 74.4 | 61.4 | 17.5 | 10.3 |
| Keratometric + pachymetric data | 0.45 | 0.752 | 54.3 | 41.2 | 24.0 | 10.3 |
| Three-model structure | | | | | | |
| Elevation + surface indices + keratometric data | 0.68 | 0.952 | 97.7 | 84.6 | 13.4 | 10.3 |
| Elevation + surface indices + pachymetric data | 0.64 | 0.936 | 93.8 | 80.8 | 13.9 | 10.3 |
| Elevation + keratometric + pachymetric data | 0.6 | 0.926 | 96.1 | 78.7 | 18.1 | 10.3 |
| Surface indices + keratometric + pachymetric data | 0.6 | 0.926 | 87.6 | 78.9 | 9.9 | 10.3 |

$R^2$, Nagelkerke Pseudo $R^2$; AUC, area under the curve; LR, likelihood ratio

using the Galilei analyzer. The cutoff points provided in the present study can be used in clinical settings, particularly among refractive surgery candidates for keratoconus screening.

Moreover, the ability of these measurements to distinguish subclinical keratoconus and keratoconus from normal individuals was investigated using the area under the ROC curves as well as logistic regression analysis. The majority of parameters had sufficient strength (AUC > 0.80) to differentiate keratoconus which can be diagnosed in 100% of cases using either surface indices or elevation parameters. Meanwhile, the overall predictive accuracy of these readings was moderate for eyes with subclinical keratoconus (AUC < 0.80) and a single set of parameters failed to completely differentiate subclinical keratoconus from normal. Therefore, several model structures were analyzed and a 3-factor model incorporating keratometric variables, elevation parameters, and surface indices turned out to be the most effective structure for screening of subclinical keratoconus which showed the highest, but still suboptimal predictive accuracy (68%).

The above-mentioned observations indicate that conventional corneal topography is adequate for the diagnosis of keratoconus and the addition of pachymetric and elevation data may not further increase the precision of detecting this condition. This means when keratoconus is diagnosed on the basis of abnormal slit-lamp findings, topographic data derived from Placido disk-based topography can confirm the diagnosis and there is no need for more sophisticated or expensive examinations such as Orbscan, or Galilei.

In sharp contrast, one needs different data sets including elevation and keratometric parameters, and surface indices for the diagnosis of subclinical keratoconus. However, such a large number of variables can be confusing, necessitating a stepwise approach for more accurate interpretation of the data.

The parameters emergeing from CRT analysis in the current study follow a type of logic which can be used by clinicians to narrow the possibilities of differential diagnosis. CRT analysis showed that SAI > 1.28 did reliably differentiate keratoconus from normal as only one (1.8%) eye in the normal group had this parameter exceeding 1.28. This observation is in good agreement with other studies reporting that deformation occurs in the anterior corneal surface of keratoconus eyes.[20-24] The radius of posterior BFS in layer 2 was the second variable present in the CRT analyses which can effectively differentiate subclinical keratoconus from normal cornea; a value ≤6.175 mm strongly suggested subclinical keratoconus and in combination with SAI > 1.28 could separate 73.9% of cases with this condition. In this regard, the CRT analysis is congruent with previous studies which demonstrate that manifestations of keratoconus occur at the posterior corneal surface in early stages of the disease, resulting in significantly steep best-fit sphere values.[1,2,17] Since, the sample size in the subclinical keratoconus group was small, the CRT analysis could not further categorize other potential predictors until maximal classification is achieved. Conducting a similar study on a larger sample size could help determine the role that other parameters may play in screening for this condition.

To the best of our knowledge, only one study has reported concerns about the performance of the dual Scheimpflug analyzer in eyes with subclinical and clinical keratoconus. Smadja et al[25] used 55 parameters (curvature, elevation, pachymetric, and wavefront parameters) derived from anterior and posterior corneal measurements to develop a method for automating the detection of subclinical and clinical keratoconus based on a tree classification. Using this decision tree classifier, they could differentiate keratoconus from normal corneas with 100% sensitivity and 99.5% specificity, and forme fruste keratoconus from normal with 93.6% sensitivity and 97.2% specificity. The most discriminant variable

to differentiate keratoconus from normal was related to the posterior asphericity asymmetry, the asphericity asymmetry index, with a cutoff value of 34.5 mm. The most discriminant variable to differentiate forme fruste keratoconus from normal was also related to posterior asphericity asymmetry, the asphericity asymmetry index, with a cutoff value of 21.5 mm. Differences observed between the above-mentioned study and ours may be explained by the criteria used for the diagnosis of subclinical/forme fruste keratoconus. In the study by Smadja et al,[25] forme fruste group were defined as eyes for which there was clinically evident keratoconus in the fellow eye. These eyes had no clinical signs of keratoconus, had normal topographic features with no asymmetric bowtie and no focal or inferior steepening pattern. However, we developed our own criteria enrolling normal appearing corneas with abnormal topographic patterns. Therefore, the difference in the selected samples makes it impossible to compare the results of these two studies.

Several indices and artificial intelligence methods, such as the Rabinowitz-McDonnell test, the KISA% index, the Klyce-Maeda-Smolek Expert system, and the corneal navigator have been developed to help diagnose keratoconus.[26-31] Using the Galilei dual Scheimpflug analyzer, we introduce a logical approach to corneal tomography parameters derived from this device. We also evaluated whether this approach can effectively differentiate corneas with subclinical keratoconus and keratoconus from normal corneas. This opens the possibility to create artifical intelligence indices from different parameters representing corneal elevation, keratometry, thickness and surface indices for the diagnosis of subclinical and clinical keratoconus.

## Financial Support and Sponsorship

Nil.

## Conflicts of Interest

There are no conflicts of interest.

## *REFERENCES*

1. de Sanctis U, Loiacono C, Richiardi L, Turco D, Mutani B, Grignolo FM. Sensitivity and specificity of posterior corneal elevation measured by Pentacam in discriminating keratoconus/subclinical keratoconus. *Ophthalmology* 2008;115:1534-1539.
2. Schlegel Z, Hoang-Xuan T, Gatinel D. Comparison of and correlation between anterior and posterior corneal elevation maps in normal eyes and keratoconus-suspect eyes. *J Cataract Refract Surg* 2008;34:789-795.
3. Jafri B, Li X, Yang H, Rabinowitz YS. Higher order wavefront aberrations and topography in early and suspected keratoconus. *J Refract Surg* 2007;23:774-781.
4. Wilson SE, Klyce SD. Screening for corneal topographic abnormalities before refractive surgery. *Ophthalmology* 1994;101:147-152.
5. Ambrósio R Jr., Klyce SD, Wilson SE. Corneal topographic and pachymetric screening of keratorefractive patients. *J Refract Surg* 2003;19:24-29.
6. Nesburn AB, Bahri S, Salz J, Rabinowitz YS, Maguen E, Hofbauer J, et al. Keratoconus detected by videokeratography in candidates for photorefractive keratectomy. *J Refract Surg* 1995;11:194-201.
7. Varssano D, Kaiserman I, Hazarbassanov R. Topographic patterns in refractive surgery candidates. *Cornea* 2004;23:602-607.
8. Seiler T, Quurke AW. Iatrogenic keratectasia after LASIK in a case of forme fruste keratoconus. *J Cataract Refract Surg* 1998;24:1007-1009.
9. Rabinowitz YS. Videokeratographic indices to aid in screening for keratoconus. *J Refract Surg* 1995;11:371-379.
10. Levy D, Hutchings H, Rouland JF, Guell J, Burillon C, Arné JL, et al. Videokeratographic anomalies in familial keratoconus. *Ophthalmology* 2004;111:867-874.
11. Swartz T, Marten L, Wang M. Measuring the cornea: The latest developments in corneal topography. *Curr Opin Ophthalmol* 2007;18:325-333.
12. Konstantopoulos A, Hossain P, Anderson DF. Recent advances in ophthalmic anterior segment imaging: A new era for ophthalmic diagnosis? *Br J Ophthalmol* 2007;91:551-557.
13. Jafarinasab MR, Feizi S, Karimian F, Hasanpour H. Evaluation of corneal elevation in eyes with subclinical keratoconus and keratoconus using Galilei double Scheimpflug analyzer. *Eur J Ophthalmol* 2013;23:377-384.
14. Karimian F, Feizi S, Doozandeh A, Faramarzi A, Yaseri M. Comparison of corneal tomography measurements using Galilei, Orbscan II, and Placido disk-based topographer systems. *J Refract Surg* 2011;27:502-508.
15. Karimian F, Feizi S, Faramarzi A, Doozandeh A, Yaseri M. Evaluation of corneal pachymetry measurements by Galilei dual Scheimpflug camera. *Eur J Ophthalmol* 2012;22 Suppl 7:S33-S39.
16. de Sanctis U, Missolungi A, Mutani B, Richiardi L, Grignolo FM. Reproducibility and repeatability of central corneal thickness measurement in keratoconus using the rotating Scheimpflug camera and ultrasound pachymetry. *Am J Ophthalmol* 2007;144:712-718.
17. Sonmez B, Doan MP, Hamilton DR. Identification of scanning slit-beam topographic parameters important in distinguishing normal from keratoconic corneal morphologic features. *Am J Ophthalmol* 2007;143:401-408.
18. Nilforoushan MR, Speaker M, Marmor M, Abramson J, Tullo W, Morschauser D, et al. Comparative evaluation of refractive surgery candidates with Placido topography, Orbscan II, Pentacam, and wavefront analysis. *J Cataract Refract Surg* 2008;34:623-631.
19. Rao SN, Raviv T, Majmudar PA, Epstein RJ. Role of Orbscan II in screening keratoconus suspects before refractive corneal surgery. *Ophthalmology* 2002;109:1642-1646.
20. Fam HB, Lim KL. Corneal elevation indices in normal and keratoconic eyes. *J Cataract Refract Surg* 2006;32:1281-1287.
21. Quisling S, Sjoberg S, Zimmerman B, Goins K, Sutphin J. Comparison of Pentacam and Orbscan IIz on posterior curvature topography measurements in keratoconus eyes. *Ophthalmology* 2006;113:1629-1632.
22. Miháltz K, Kovács I, Takács A, Nagy ZZ. Evaluation of keratometric, pachymetric, and elevation parameters of keratoconic corneas with Pentacam. *Cornea* 2009;28:976-980.
23. Tomidokoro A, Oshika T, Amano S, Higaki S, Maeda N, Miyata K. Changes in anterior and posterior corneal curvatures in keratoconus. *Ophthalmology* 2000;107:1328-1332.
24. Emre S, Doganay S, Yologlu S. Evaluation of anterior segment parameters in keratoconic eyes measured with the Pentacam system. *J Cataract Refract Surg* 2007;33:1708-1712.
25. Smadja D, Touboul D, Cohen A, Doveh E, Santhiago MR, Mello

GR, et al. Detection of subclinical keratoconus using an automated decision tree classification. *Am J Ophthalmol* 2013;156:237-246.e1.

26. Rabinowitz YS. Keratoconus. *Surv Ophthalmol* 1998;42:297-319.
27. Rabinowitz YS, McDonnell PJ. Computer-assisted corneal topography in keratoconus. *Refract Corneal Surg* 1989;5:400-408.
28. Maeda N, Klyce SD, Smolek MK, Thompson HW. Automated keratoconus screening with corneal topography analysis. *Invest Ophthalmol Vis Sci* 1994;35:2749-2757.
29. Smolek MK, Klyce SD. Current keratoconus detection methods compared with a neural network approach. *Invest Ophthalmol Vis Sci* 1997;38:2290-2299.
30. Rabinowitz YS, Rasheed K. KISA% index: A quantitative videokeratography algorithm embodying minimal topographic criteria for diagnosing keratoconus. *J Cataract Refract Surg* 1999;25:1327-1335.
31. Klyce SD, Karon MD, Smolek MK. Screening patients with the corneal navigator. *J Refract Surg* 2005;21 5 Suppl: S617-S622.